

Percolation conductivity in hafnium sub-oxides

D. R. Islamov, V. A. Gritsenko, C. H. Cheng, and A. Chin

Citation: [Applied Physics Letters](#) **105**, 262903 (2014); doi: 10.1063/1.4905308

View online: <http://dx.doi.org/10.1063/1.4905308>

View Table of Contents: <http://scitation.aip.org/content/aip/journal/apl/105/26?ver=pdfcov>

Published by the [AIP Publishing](#)

Articles you may be interested in

[Ab initio modeling of oxygen-vacancy formation in doped-HfO_x RRAM: Effects of oxide phases, stoichiometry, and dopant concentrations](#)

Appl. Phys. Lett. **107**, 013504 (2015); 10.1063/1.4926337

[The origin of 2.7 eV luminescence and 5.2 eV excitation band in hafnium oxide](#)

Appl. Phys. Lett. **104**, 071904 (2014); 10.1063/1.4865259

[Role of point defects and HfO₂/TiN interface stoichiometry on effective work function modulation in ultra-scaled complementary metal–oxide–semiconductor devices](#)

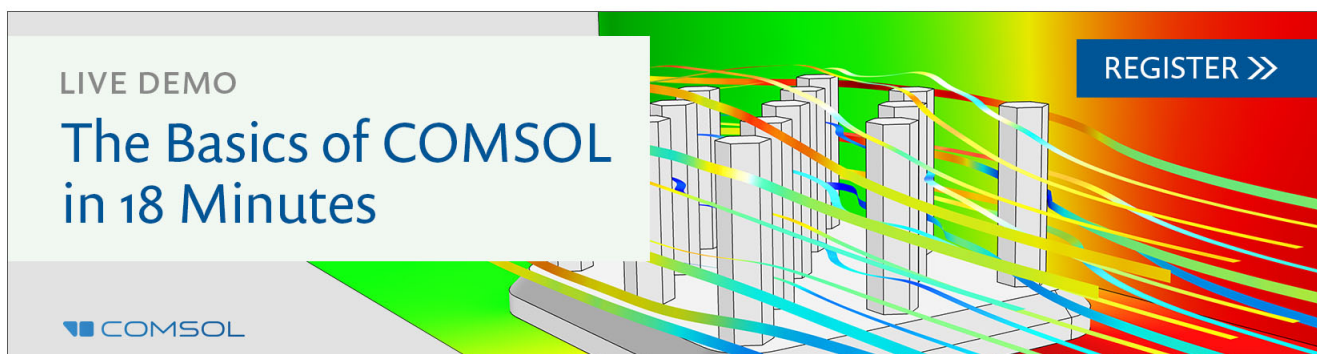
J. Appl. Phys. **114**, 034505 (2013); 10.1063/1.4816090

[Quantum-size effects in hafnium-oxide resistive switching](#)

Appl. Phys. Lett. **102**, 183505 (2013); 10.1063/1.4802265

[Structure and electronic properties of zirconium and hafnium nitrides and oxynitrides](#)

J. Appl. Phys. **97**, 044108 (2005); 10.1063/1.1851000

The advertisement features a 3D bar chart with several vertical bars of varying heights. Overlaid on the chart are several colorful, flowing lines in shades of green, yellow, orange, and red, suggesting data analysis or simulation results. The background is a gradient from green to red. A white box on the left contains the text 'LIVE DEMO' and 'The Basics of COMSOL in 18 Minutes'. The COMSOL logo is in the bottom left corner. A blue button with white text 'REGISTER >>' is in the top right corner.

LIVE DEMO

The Basics of COMSOL in 18 Minutes

COMSOL

REGISTER >>

Percolation conductivity in hafnium sub-oxides

D. R. Islamov,^{1,2,a)} V. A. Gritsenko,^{1,2,b)} C. H. Cheng,³ and A. Chin^{4,c)}

¹Rzhanov Institute of Semiconductor Physics, Siberian Branch of Russian Academy of Sciences, Novosibirsk 630090, Russian Federation

²Novosibirsk State University, Novosibirsk 630090, Russian Federation

³Department of Mechatron Technology, National Taiwan Normal University, Taipei 106, Taiwan

⁴National Chiao Tung University, Hsinchu 300, Taiwan

(Received 4 September 2014; accepted 18 December 2014; published online 30 December 2014)

In this study, we demonstrated experimentally that formation of chains and islands of oxygen vacancies in hafnium sub-oxides (HfO_x , $x < 2$) leads to percolation charge transport in such dielectrics. Basing on the model of Éfros-Shklovskii percolation theory, good quantitative agreement between the experimental and theoretical data of current-voltage characteristics was achieved. Based on the percolation theory suggested model shows that hafnium sub-oxides consist of mixtures of metallic Hf nano-scale clusters of 1–2 nm distributed onto non-stoichiometric HfO_x . It was shown that reported approach might describe low resistance state current-voltage characteristics of resistive memory elements based on HfO_x . © 2014 AIP Publishing LLC. [<http://dx.doi.org/10.1063/1.4905308>]

Hafnium oxide (hafnia, HfO_2) and sub-oxides (HfO_x , $x < 2$) play extremely important roles in modern microelectronics. Hafnia is used in modern MOSFETs as high- κ gate dielectric with low leakage currents.^{1–4} Hafnium sub-oxides are the most promising materials to be used as active medium in resistive random access memory (RRAM),^{5,6} which might be used for universal memory combining the most favorable properties of both high-speed dynamic random access memory and non-volatile flash memory.^{7–11} RRAM has many advantages: a simple metal-insulator-metal (MIM) structure, a small memory cell, potential for 3D integration, high read and write operation speeds, low power consumption, and the ability to store information over the long term.¹² A RRAM operation is principally based on switching back and forth from the insulating medium's high resistance state (HRS) to a low resistance state (LRS) when a current flows. Conductivity of HfO_x used as RRAM active medium is limited by ionization of charge carrier traps when RRAM is switched to the HRS state.^{6,13,14} Unfortunately, unlike the flash memory, the fundamental physics mechanism of RRAM is still inadequate but that is vital to realize the ultra-low-power memory array.

In this letter, we report that the charge transport mechanism is described in terms of percolation theory when hafnium-sub-oxides-based RRAM is switched to the LRS state.

Transport measurements were recorded for MIM structures of Si/TaN/ HfO_x /Ni. To fabricate these structures, we deposited the 8-nm-thick amorphous HfO_x on 100-nm-thick TaN films on Si wafers, using physical vapor deposition. A pure HfO_2 target was bombarded by an electron beam, and HfO_2 was deposited on the wafer. No post deposition annealing was applied to produce highly non-stoichiometric HfO_x films. Structural analysis showed that the resulting films were amorphous. All samples for transport measurements

were equipped with round 50-nm-thick Ni gates with a radius of 70 μm .

Transport measurements were performed using a Hewlett Packard 4155B semiconductor parameter analyzer and an Agilent E4980A precision LCR meter. All measurement equipments were protected against short circuiting with the current through the sample limitation of 1 μA .

The most commonly used LRS description in RRAM structures consists of conductive filament (CF), approximately 1–10 nm in diameter.^{15–17} The CF forming is caused by charged ion movements due to temperature gradients and electric fields.¹⁷ It was supposed that CFs in Ni/ HfO_2 /Si RRAM structures consist of nickel, migrated from the metal electrode,¹⁶ but these assumptions were based on results of RRAM measurements in Ni/NiO/Ni-type structures (i.e., with NiO dielectric medium with Ni electrodes). However, CF has metallic temperature dependence of resistance

$$(R - R_0) \propto (T - T_0) \quad (1)$$

(here R_0 is the CF resistance at temperature T_0), with average resistivity in three orders smaller than resistivity of pure Hf metal.¹⁵

Experimental current-voltage characteristics (I - V) in Si/TaN/ HfO_x /Ni MIM structures at different temperatures are shown in Fig. 1 by colored characters. The measured current in LRS has strong exponential dependence on voltage and temperature. Expected current through non-stoichiometric HfO_x CF¹⁵ (dark cyan dotted line in Fig. 1) is close to experiment results, but expected values are large for temperatures of $T = 25$ – 50 °C, and lower than measured at $T = 85$ °C. The current grows exponentially with temperature growing, while following results from the literature, the current should decrease with the temperature increasing (1).

Therefore, we suppose that LRS conductivity is conditioned by the presence of a non-stoichiometric HfO_x islands in HfO_2 matrix as HfO_y with $y \lesssim 1.89$ splits into phases of Hf, HfO_x , and HfO_2 .¹⁸ The overview on the structure of non-stoichiometric sub-oxides and sub-nitrides was developed for SiO_x , SiN_x , and SiO_xN_y .^{19–22}

^{a)}Electronic mail: damir@isp.nsc.ru

^{b)}Electronic mail: grits@isp.nsc.ru

^{c)}Electronic mail: albert_achin@hotmail.com

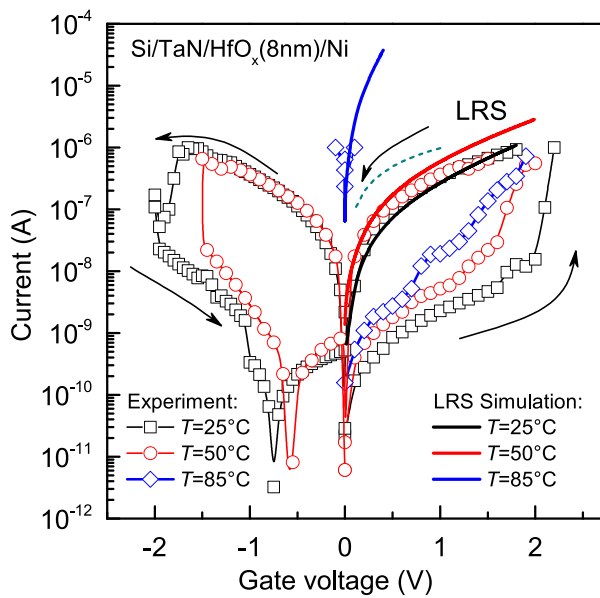


FIG. 1. Experimental RRAM current-voltage characteristics hysteresis (characters) in Si/TaN/HfO_x/Ni MIM structures at different temperatures. Black, red, and blue solid lines present LRS simulations in terms of percolation model. Dark cyan dotted line models I - V of sub-stoichiometric HfO_x CF.¹⁵

A 2D structural image of non-stoichiometric HfO_x, regarding the intermediate structural model,²⁰ is presented in Fig. 2(a). According to this model, the CF in hafnium suboxide consists of a mixture of metallic hafnium nanoscale clusters (blue drops) and non-stoichiometric HfO_x (green

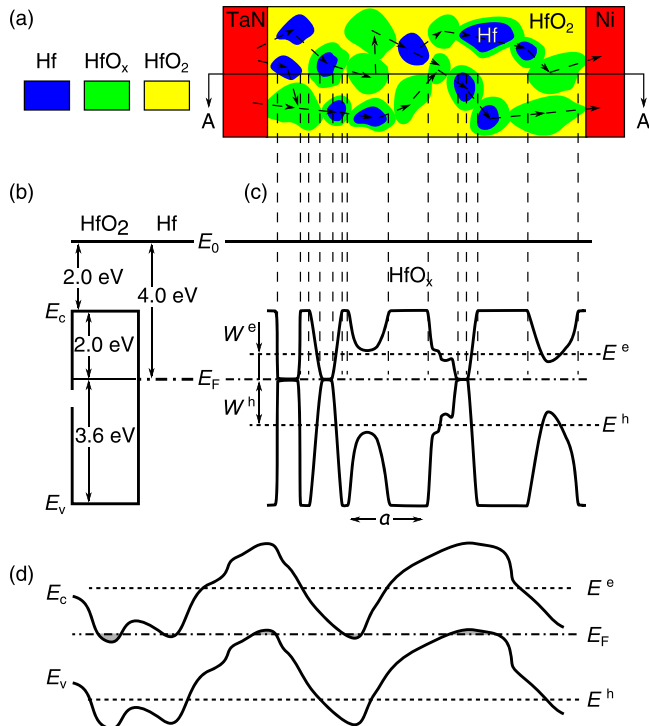


FIG. 2. Percolation model in electron systems with the nanoscale potential fluctuations. (a) Schematic planar illustration of Hf/HfO_x ($x < 2$) space-modulated by chemical composition structure. (b) Flat band energy diagram of HfO₂/Hf structure. (c) Energy diagram of the structure with nanoscale potential fluctuations. (d) Energy diagram of large-scale potential fluctuations in a semiconductor layer.²⁴ $E^{e,h}$ and $W^{e,h}$ are percolation levels and percolation thresholds of the electrons and holes, respectively.

islands) distributed onto HfO₂ matrix (yellow area). Fig. 2(c) is an energy diagram of HfO_x in the intermediate structural model. According to this plot, spatial fluctuations in the chemical composition of HfO_x lead to local band gap width spatial fluctuations. The maximal fluctuation of the energy scale is equal to the HfO₂ band gap width of $E_g = 5.6$ eV.²³ The work function of metallic hafnium is 4.0 eV. The maximal fluctuation scale of the HfO_x conduction band is 2.0 eV, which equals the electron barrier height of Hf/HfO₂ interface. The hole energy barrier of Hf/HfO₂ is 3.6 eV (Fig. 2(b)), which leads to the maximal fluctuation scale of the HfO_x valence band of 3.6 eV.

The nanoscale fluctuations at the bottom of conduction band E_c and at the top of valence band E_v are close to those proposed in the model developed in Refs. 24 and 25, as shown in Fig. 2(d). The charge transport in such electron systems can be described according to percolation. This model assumes that excited electrons with energy higher than the flow level E^e are delocalized, and driving round a random potential, transfer the charge. The hole conductivity is realized through the excitation of electrons with energy E^h to the Fermi level. These excitations form hole-type quasiparticles, which transfer the charge. In other words, to be involved in transport processes, electrons and holes must overcome energy thresholds ($W^{e,h}$ here, and $W^e \neq W^h$, in general). The current-voltage characteristics are exponentials²⁴

$$I(T) = I_0(T) \exp\left(\frac{(CeFaV_0^\nu)^{\frac{1}{1+\nu}}}{kT}\right), \quad (2)$$

where I is the current, I_0 is the preexponential factor, e is the electron charge, F is the electric field, a is the space scale of fluctuations, V_0 is the amplitude of energy fluctuation, k is the Boltzmann constant, C is a numeric constant, and ν is a critical index. The values of the constants were derived from Monte-Carlo simulations and evaluated at $C \simeq 0.25$ (Ref. 24) and $\nu = 0.9$.²⁵ Percolation energy threshold W can be evaluated based on the temperature dependency of the preexponential factor

$$I_0(T) \sim \exp\left(-\frac{W}{kT}\right). \quad (3)$$

The solid colored lines in Fig. 1 indicate the results of LRS simulations regarding the percolation model, given in (2). Numeric fitting returns the value of combination as $CaV_0^{0.9} = 0.45 \text{ nm} \cdot \text{eV}^{0.9}$, which corresponds to $V_0 = 1.9$ eV when $a = 1$ nm and $C = 0.25$. The slope of a fitting line in a $\ln(I_0)$ -vs- T^{-1} plate according to (3) corresponds to a percolation threshold of $W \approx 1.0$ eV. Because $W \leq V_0 \leq 2.0$ eV (for electrons), we can estimate the space size of nanoscale fluctuations as $a \approx 1$ –2 nm.

Previous experiments in charge transfer have demonstrated that hafnia conductivity is bipolar (or two-band).^{4,26–28} electrons are injected from a negatively shifted contact in the dielectric, and holes are injected from a positively shifted electrode in the dielectric. In our model, LRS conductivity can also be studied using electrons and holes. For the reason of simplicity, the current study was limited for considering monopolar electron conductivity.

The results demonstrate that charge transport in non-stoichiometric hafnium sub-oxides is described according to the percolation model in electron systems exhibiting potential nanoscale fluctuations. This approach can be applied to explain RRAM in GeO_x - and SiO_x -based structures.^{29,30}

This work was partly supported by National Science Council, Taiwan (Grant No. NSC103-2923-E-009-002-MY3) (growing test structures, preparing samples, and performing transport measurements) and by the Russian Science Foundation (Grant No. 14-19-00192) (calculations and modeling).

¹Z. Xu, M. Houssa, R. Carter, M. Naili, S. D. Gendt, and M. Heyns, *J. Appl. Phys.* **91**, 10127 (2002).

²T. P. Ma, H. M. Bu, X. W. Wang, L. Y. Song, W. He, M. Wang, H.-H. Tseng, and P. J. Tobin, *IEEE Trans. Device Mater. Reliab.* **5**, 36 (2005).

³J. Robertson, *Rep. Prog. Phys.* **69**, 327 (2006).

⁴L. Vandelli, A. Padovani, L. Larcher, R. G. Southwick, W. B. Knowlton, and G. Bersuker, *IEEE Trans. Electron Devices* **58**, 2878 (2011).

⁵L. Goux, P. Czarniecki, Y. Y. Chen, L. Pantisano, X. P. Wang, R. Degraeve, B. Govoreanu, D. J. Jurczak, M. Wouters, and L. Altimime, *Appl. Phys. Lett.* **97**, 243509 (2010).

⁶Z. Wang, H. Y. Yu, X. A. Tran, Z. Fang, J. Wang, and H. Su, *Phys. Rev. B* **85**, 195322 (2012).

⁷D. B. Strukov, G. S. Snider, D. R. Stewart, and R. S. Williams, *Nature* **453**, 80 (2008).

⁸J. J. Yang, M. D. Pickett, X. Li, D. A. A. Ohlberg, D. R. Stewart, and R. S. Williams, *Nat. Nanotechnol.* **3**, 429 (2008).

⁹M.-J. Lee, S. Han, S. H. Jeon, B. H. Park, B. S. Kang, S.-E. Ahn, K. H. Kim, C. B. Lee, C. J. Kim, I.-K. Yoo, D. H. Seo, X.-S. Li, J.-B. Park, J.-H. Lee, and Y. Park, *Nano Lett.* **9**, 1476 (2009).

¹⁰J. Borghetti, G. S. Snider, P. J. Kuekes, J. J. Yang, D. R. Stewart, and R. S. Williams, *Nature* **464**, 873 (2010).

¹¹M.-J. Lee, C. B. Lee, D. Lee, S. R. Lee, M. Chang, J. H. Hur, Y.-B. Kim, C.-J. Kim, D. H. Seo, S. Seo, U.-I. Chung, I.-K. Yoo, and K. Kim, *Nat. Mater.* **10**, 625 (2011).

¹²C.-H. Cheng, F.-S. Yeh, and A. Chin, *Adv. Mater.* **23**, 902 (2011).

¹³S. D. Ganichev, E. Ziemann, W. Prettl, I. N. Yassievich, A. A. Istratov, and E. R. Weber, *Phys. Rev. B* **61**, 10361 (2000).

¹⁴D. R. Islamov, V. A. Gritsenko, C. H. Cheng, and A. Chin, *Appl. Phys. Lett.* **105**, 222901 (2014), e-print [arXiv:1409.6887](https://arxiv.org/abs/1409.6887).

¹⁵G. Bersuker, D. C. Gilmer, D. Veksler, P. Kirsch, L. Vandelli, A. Padovani, L. Larcher, K. McKenna, A. Shluger, V. Iglesias, M. Porti, and M. Nafria, *J. Appl. Phys.* **110**, 124518 (2011).

¹⁶T.-H. Hou, K.-L. Lin, J. Shieh, J.-H. Lin, C.-T. Chou, and Y.-J. Lee, *Appl. Phys. Lett.* **98**, 103511 (2011).

¹⁷S. Ambrogio, S. Balatti, D. C. Gilmer, and D. Ielmini, *IEEE Electron Device Lett.* **61**, 2378 (2014).

¹⁸V. N. Kruchinin, T. V. Perevalov, V. S. Aliev, V. A. Shvets, D. R. Islamov, V. A. Gritsenko, and I. P. Prosvirin, "Nanoscale Potential Fluctuation in Non-Stoichiometric HfO_x " (unpublished).

¹⁹K. Hübner, *J. Non-Cryst. Solids* **35–36**(Part 2), 1011 (1980).

²⁰Y. N. Novikov and V. A. Gritsenko, *J. Appl. Phys.* **110**, 014107 (2011).

²¹V. A. Gritsenko, R. Kwok, H. Wong, and J. B. Xu, *J. Non-Cryst. Solids* **297**, 96 (2002).

²²V. A. Gritsenko, J. B. Xu, R. W. M. Kwok, Y. H. Ng, and I. H. Wilson, *Phys. Rev. Lett.* **81**, 1054 (1998).

²³V. Afanas'ev, *Internal Photoemission Spectroscopy: Principles and Applications* (Elsevier Science, Amsterdam, 2008), p. 312.

²⁴B. I. Shklovskii, *Sov. Phys. Semicond.* **13**, 53 (1979).

²⁵B. I. Shklovskii and A. L. Éfros, *Phys.-Usp.* **18**, 845 (1975).

²⁶D. R. Islamov, V. A. Gritsenko, C. H. Cheng, and A. Chin, *Appl. Phys. Lett.* **99**, 072109 (2011).

²⁷T. Ando, N. D. Sathaye, K. V. R. M. Murali, and E. A. Cartier, *IEEE Electron Device Lett.* **32**, 865 (2011).

²⁸Y. N. Novikov, *J. Appl. Phys.* **113**, 024109 (2013).

²⁹A. V. Shaposhnikov, T. V. Perevalov, V. A. Gritsenko, C. H. Cheng, and A. Chin, *Appl. Phys. Lett.* **100**, 243506 (2012).

³⁰A. Mehonic, S. Cuff, M. Wojdak, S. Hudziak, O. Jambois, C. Labb, B. Garrido, R. Rizk, and A. J. Kenyon, *J. Appl. Phys.* **111**, 074507 (2012).